TECHNICAL REPORT NO. 15

SLUG FLOW

BY

Peter Griffith

Grahm B. Wallis

For

The Office of Naval Research

NONR-1841(39)

DSR PROJECT NO. 7-7673

May 1959

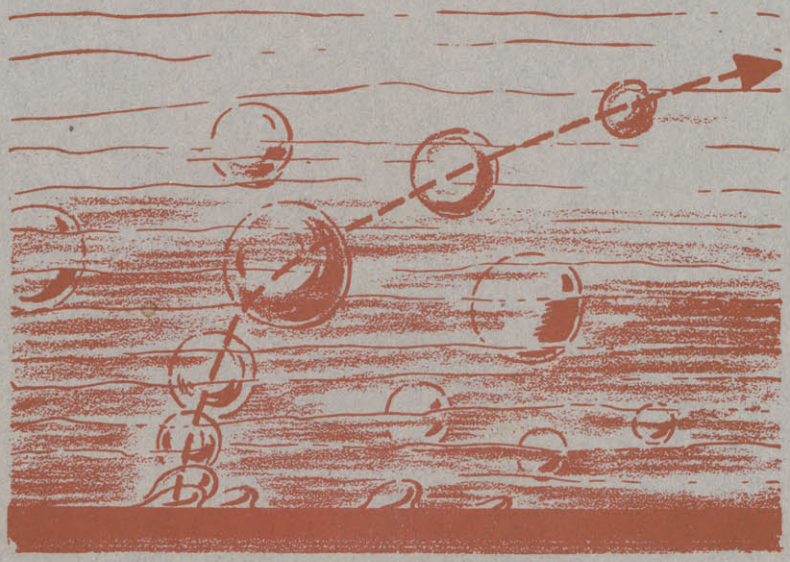

DIVISION OF SPONSORED RESEARCH

MASSACHUSETTS INSTITUTE OF TECHNOLOGY

CAMBRIDGE, MASSACHUSETTS

Technical Report No. 15

Slug Flow

by

Peter Griffith*

Graham Wallis**

For

The Office of Naval Research

Nonr 1841(39)

DSR Project No. 7-7673

1 May 1959

Division of Sponsored Research
Massachusetts Institute of Technology
Cambridge, Massachusetts

* Assistant Professor of Mechanical Engineering, M.I.T.

** Research Assistant, Department of Mechanical Engineering, M.I.T.

Slug Flow

INTRODUCTION

When two phases flow concurrently in a pipe, they can distribute themselves in a number of different configurations. The gas could be uniformly dispersed throughout the liquid in the form of small bubbles. There could be large gas bubbles almost filling the tube. There could be an annulus of liquid and core of vapor with or without drops of liquid in it. The interface could be smooth or wavy. When one describes how the phases are distributed, one is specifying the flow regime. Such a description is necessary before any mathematical model can be constructed which will predict a quantity such as pressure drop.

It is naive to expect that a single mathematical model would adequately encompass all possible two-phase flow regimes, even for a single geometric configuration. Therefore, we shall begin by saying that for this work the results that have been obtained and the conclusions that have been drawn apply only to fully developed slug flow in a round vertical pipe.

Slug flow is characterized by large bubbles, almost filling the tube, which are separated by slugs of liquid. The nose of the bubble is rounded and the tail generally flat. One may or may not find small bubbles in the slug following the large bubble. A number of typical slug flow bubbles are pictured in Figures 4-10.

Bubbles very similar to these have been studied by Dumistrescu (1), and Davis and Taylor (2). Both these references consider the same problem. How rapidly will a closed tube full of liquid empty when the bottom is suddenly opened to the atmosphere. The approach used by both authors is to assume that the asymptotic rise velocity (for large times) can be calculated from potential flow theory. The boundary condition at the pipe wall is that the velocity is axial. At the bubble boundary it is assumed that the pressure is constant. The problem is then to find the shape of the bubble that would satisfy the constant pressure boundary condition. This was done approximately and in both cases the comparison with experiment was satisfactory though the deviations became large for small tubes.

The work of Davis and Taylor, and Dumitrescu served as the starting point for this investigation. The boundary condition at the bubble wall for large bubbles, constant pressure, was still valid to an excellent approximation and the finiteness of the slug flow bubbles did not appear to make much difference in their rise velocity.

In the next section, the fluctuation period, the mean density, and the pressure drop will be expressed in terms of the pipe area, the Taylor bubble rise velocity and the flow rates of the two phases. In subsequent sections the observations rade of bubble shape, length and velocity will be described and then a comparison of computed and measured pressure drops given.

SLUG FLOW THEORY

Bubble Period

Assume as a control volume a section of vertical pipe which goes from the entrance of the pipe to the middle of one slug. Fix the control volume in space, Figure 1, line "a". Continuity will yield the result that, for both phases incompressible, the velocity in the slug well ahead of the tip of the bubble is simply the total volume flow rate divided by the pipe area.* If the velocity of the bubble is V_b with respect to the liquid ahead of it, then the velocity of the bubble with respect to the ground will be

$$\frac{Q_f + Q_g}{A_p} + V_b$$

The time it takes for a representative sample, that is a bubble and slug, to pass a given section of the pipe will be

$$\Delta t = \frac{(L_s + L_b)A_p}{Q_f + Q_g + V_b A_p} \qquad (1)$$

Δt is then the period for the bubbles.

Average Density

Let us continue by considering the time average flow rate of the gas phase past a section. During one period one bubble of volume $\mathcal{V}_b$ will pass; therefore, the average flow rate for the gas will be

$$Q_g = \frac{\mathcal{V}_b}{\Delta t} \qquad (2)$$

The average density in a volume containing two phases is

$$\rho_a = \rho_f \left[1 - \frac{\mathcal{V}_g}{\mathcal{V}}\right] + \left[\rho_g \frac{\mathcal{V}_g}{\mathcal{V}}\right] \qquad (3)$$

---

* It can be shown by a more complete analysis that the present formulation also holds for a compressible gas.

In terms of the phase densities, the average density of a typical pipe section containing one bubble and one slug will be

$$\rho_a = \rho_f \left[1 - \frac{\mathcal{V}_b}{(L_s + L_b)A_p}\right] + \rho_g \left[\frac{\mathcal{V}_b}{(L_s + L_b)A_p}\right] \tag{4}$$

When equation (1) is substituted into (2) and the result substituted into (4), one obtains:

$$\rho_a = \rho_f \left[\frac{Q_f + V_b A_p}{Q_f + Q_g + V_b A_p}\right] + \frac{\rho_g Q_g}{Q_f + Q_g + V_b A_p} \tag{5}$$

This is the desired expression.

Pressure Drop

If one considers a typical section of pipe which contains one slug and one bubble, and takes a control volume moving with the bubbles at bubble velocity, it is obvious from symmetry considerations that the momentum fluxes in and out are identical. Such a control volume is illustrated in Figure 1, control volume "b". Therefore, the pressure drop between sections 1 and 2 is

$$(P_1 - P_2)A_p - \rho_a g (L_s + L_b)A_p - \tau_w A_w = 0 \tag{6}$$

For many applications, the shear stress term is much less significant than the gravity term so that to a good approximation the time average pressure gradient at a point becomes

$$\frac{\Delta P}{\Delta L} = \rho_a g \tag{7}$$

Bubble Length and Slug Length

Let us assume that an approximate empirical formula relating bubble length to volume exists in the following form

$$\mathcal{V}_b = A_p(m L_b - n D_p) \tag{8}$$

Such a formula has been fitted to the calculated shape of Dumitrescu, which is valid only for the potential flow case. However, such a formula could as well be fitted to any bubble whether the conditions of potential flow are satisfied or not. The constants "m" and "n" would simply be somewhat different.

If one fixes the slug length, the bubble length is fixed by continuity considerations on the gas phase and the ratio of gas to liquid flow. Let us suppose that the slug length is specified and the relation between bubble length and volume is that of Equation (8). Substituting (1) and (8) into (2) results in this expression for bubble length

$$L_b = \frac{Q_g L_s + n D_p(Q_g + Q_f + V_b A_p)}{m(Q_g + Q_f + V_b A_p) - Q_g} \tag{9}$$

This equation relates to bubble length to the slug length and various other known quantities.

The above equation is interesting in that, for certain values of the parameters, the denominator goes to 0. That is, the bubble length becomes infinite. In principle this might provide an explanation for the transition to annular flow.

Bubble Volume

As long as the bubble volume vs. length relationship is adequately represented by a formula of the type of equation (8), equation (9) is valid. For the particular case of potential flow around the bubble the constants in equation (8) can be evaluated and are

$$m = 0.913$$
$$n = 0.526$$

for $2 < L/D < 20$

Though the shape must be altered if the flow around the bubble is not irrotational, it appears as though the above values for "m" and "n" work quite well whether the flow is irrotational or not. That is, the bubble shape is relatively insensitive to conditions in the liquid.

APPARATUS

A diagram of the apparatus is shown in Fig. 2.

The central feature is the 18 ft. vertical tube in which flow studies are made. This tube is made of three 6 ft. sections of plexiglass tubing which are finished flat at the ends and are joined together to form the continuous length by gluing them firmly into plexiglass blocks which have been drilled out to fit the outside diameter of the tube.

The uppermost 6 ft. section carries six pressure taps at one foot intervals and these are connected to vertical water manometers. Hose clamps are used in the connecting lines so that the manometers may either be isolated or the flow to them suitably throttled to damp out pressure fluctuations. The tubes leading from each pressure tap to the corresponding manometer slant downwards. This prevents air bubbles from entering the manometer and making accurate readings impossible.

Near its upper end the main tube passes through a block which is used to anchor it to the wooden board supports. A flexible hose connects the top end of the tube to the discharge tank in which air and water are separated. This tank is drained by a further length of hose which feeds weigh-buckets as required. By inserting a small diameter flexible hose into the top of the tube, it is also possible to produce down-flow in the test section although in the normal course of events the direction of flow is upwards.

At its lower end, the tube carries a plastic block suitably drilled to provide inlet ports for the air and water supply. Air is fed through a 1/8" diameter hole inclined downwards towards the tube inlet and water is supplied through a 3/8" diameter horizontal hole. Needle valves in hot and cold water supply lines control the flow rate and water temperature. Air supply is also controlled by a needle valve in the line. Before entering the apparatus, the air passes through a filter and metering orifice plate. Three sizes of tube were used in these experiments: 1", 3/4" and 1/2" I.D.

Photographs of the flow patterns were taken in the upper half of the top tube section. Behind the tube there is a white sheet of paper which has horizontal lines drawn on it at 1/2" intervals. A 2 microsecond flash* is employed

* "Microflash" type 1530-A manufactured by General Radio, Cambridge, Mass.

and photographs are obtained on 35mm Kodak Panatomic X film. The negatives were then analyzed on a microfilm reader. Illumination is from the front, to the side and below the center line. In this way, bubbles and scale are illuminated as uniformly as possible using only one flash source.

EXPERIMENTAL TECHNIQUES AND RESULTS

Bubble Rise Velocity Experiments

Measurements of bubble rise velocities were made in both still and moving water. First, the water velocity was set by means of the needle valves. Next, a single bubble was introduced by rapid opening and closing of the air supply valve. Bubble length was between 2 and 10 diameters. Bubbles were timed with a stopwatch over a standard length of 9 ft., the first mark being 3 ft. from the inlet. An experimental limitation is the accuracy of the stopwatch (1/10 secs) so that rise times of less than 5 seconds were not found to be sufficiently accurate. Water flow rates are measured to suitable accuracy by use of a weigh-bucket. Both upward and downward flow of the water was investigated and cold and hot water was used to investigate the effects of Reynolds number.

At a given water flow rate the bubble rise velocity was found to be independent of the length once the bubble was large enough to attain the G.I. Taylor shape. Consistency of results in this respect was remarkable, involving in general only changes of the order of stopwatch accuracy between the two extremes. Apparently, the hydrodynamics at the nose of the bubble is the sole determining factor.

At first it was expected that the velocity of the air bubble relative to the mean water velocity would be independent of the stream velocity. However, a few experiments soon showed that this was not the case. The bubble velocity is appreciably altered as the stream velocity profile changes. Results for the three pipes at various water temperatures are shown in Fig. 3 and Appendix 1.

As the downflow water velocity was increased, a point was reached at which the stable character of the bubble suddenly changed. Instead of assuming the smooth steady shape of previous experiments, the nose of the bubble began to distort, to become alternately eccentric on one side or another, and to lean over to one side of the tube. As a general rule, the rise velocity would change quite randomly as the shape changed, being higher the greater the distortion of the nose. The bubble appeared quite "uncertain" which shape to assume so that readings of its velocity showed considerable variation from one experiment to the next. Finally, as downflow water velocity was further

increased, the unsymmetrical shape became dominant and the motion became steady again. The transition point is marked with a cross in the Fig. 3.

Qualitative Description of Slug Flow

With the present apparatus it is possible to cover a range of slug flows varying from the first development of this regime at the transition from bubbly flow up to conditions where the slugs are either several feet long (high quality flow) or so severely distorted by shear stress and turbulent forces that new phenomena begin to appear. Because of air supply limitations, it was impossible to obtain the transition to annular flow with this apparatus.

1" Pipe

The largest pipe provides the best illustration of normal slug flow since in its case the effects of viscosity and surface tension are least.

Under "normal slug flow conditions" the flow appears as shown in Fig. 4. A series of bubbles, just like those observed by G. I. Taylor or Dumitrescu, flow up the pipe, separated by "plugs" of water which are relatively free of bubbles. The wake of the previous bubble is smoothed out by turbulent mixing and by eddies so that its effect on the next bubble is negligible. Some small bubbles are formed in the wake by being torn off the back of the main bubble, but these soon reach an equilibrium concentration with as many being formed as are re-absorbed. The smallest bubbles formed in this way are unable to keep pace with the parent and are swept downstream, either to be absorbed by some later bubble or to coalesce among themselves until they reach sufficient size to rise with the same velocity as the large bubbles.

It should be stressed that this kind of ideal flow is only to be found over a limited range of flow rates and regions. Theoretically, slug flow is possible at almost any flowing quality, the bubble length simply adjusts accordingly. In fact, in investigating the development of slug flow from the "bubbly" flow regime, it was found that it was quite possible to have bubbly flow at the tube entrance whereas a few feet higher up chance encounters would

create a bubble sufficiently large to fill the tube and to start to grow into a typical slug flow bubble by absorbing its neighbors. By varying flow rates it was possible to extend this "entrance region" to the full 18 feet of pipe whereas it was suspected that in a longer pipe slug flow would be the ultimate stable regime. Of course, the bubbles are also growing as they rise due to the drop in hydrostatic pressure, but undoubtedly the entrance region effects predominate. See Fig. 6 which shows these effects 16 feet from pipe entrance. This effect is probably a major cause of deviations among the data of various experiments on transition from bubbly to slug flow. When this "transition" occurs, and how it is defined, is a function of the particular apparatus used, the method of gas injection, length (or perhaps better time) from injection to point of observation, and perhaps some other variables.

It is interesting to note that there is an attraction between rising bubbles which decreases rapidly with separation distance. As slug flow develops, there is a continual "sucking up" of the lower of a pair of bubbles into the upper one. Once the bubbles get closer than a few diameters this process proceeds rapidly, in times of the order of a second. The explanation for this phenomenon is that the wake of the first bubble gives rise to a water velocity profile which causes the second bubble to rise faster. A more detailed discussion of this will be presented in the next chapter.

In the 1" pipe it was possible to observe bubbles of approximately the ideal form which were 6 feet and more in length. The only noticeable way in which these bubbles differ from the shorter ones is in the increase in surface waves at the air-water interface. The skin of the bubble presents an increasingly rough appearance, presumably due to turbulence in the liquid film, and consequent capillary waves on the surface.

At higher flow rates the bubble wakes become more agitated (see Fig. 7), a larger number of small bubbles are torn off at the tail, and consequently, the whole wake becomes richer in bubbles. This results in several small bubbles being swept down as far as the following bubble. These may remain intact for some distance as they are drawn into the flow around the large bubble. The bubble interface surface becomes distorted in the neighborhood of these small bubbles.

3/4" Pipe

The phenomena observed in this 3/4" pipe are, in general, exactly parallel to those observed in the 1" pipe. Photographs were only taken in this case to obtain a certain amount of data about bubble and slug lengths.

1/2" Pipe

It is in the 1/2"pipe that the effects of surface tension begin to become pronounced. In fact the study of slug flow has to be confined to qualities and flow rates well above the bubbly flow regime because of the appearance of "bowler hat" bubbles in profusion at intermediate qualities. These hat-shaped bubbles are formed in a stream at the air inlet and flow upwards in a row. Their mutual attraction now results in the formation of several pseudo- G. I. Taylor bubbles which have the overall dimensions of normal slug flow bubbles, but which consist of a series of hat-shaped bubbles stacked closely one on top of the other. At low flow rates these bubbles do not agglomerate easily and no final smooth bubble is formed in the length of the apparatus. Figs. 8 and 9 show photographs at somewhat higher flow rates and it can be seen how some of these very rough bubbles can be present simultaneously with almost perfectly smooth G. I. Taylor bubbles. Even at higher air flows, Fig. 10, the very long G. I. Taylor bubbles still may have unabsorbed caps attached since the agglomeration rate at the nose is small.

PRESSURE DROP

Pressure drop data for all three tubes was read directly from the water manometers on the last six feet of pipe. It was checked that the pressure drop was linear and steady over the six pressure taps and then the pressure difference between first and last was recorded. Results are shown in the table of results (Appendix 2). Pressure fluctuations were kept to a minimum when necessary, by adjusting the hose clamps.

BUBBLE AND SLUG LENGTHS

Lengths of bubbles and slugs were read directly off the 35mm negatives using a microfilm viewer. For each experiment a full 36 exposure roll of film was used, each exposure covering three feet of pipe. This gave enough readings in the case of the 1/2" pipe for the results to be plotted in histogram form (Fig. 11). In the case of the 1" pipe, there was not enough data for a statistical approach to be worthwhile so only average lengths are quoted in the results. As a check on the bubble-slug length ratio, measurements were taken of the fraction of a standard 10" length occupied by bubbles and averaged. Results are shown in Appendix 2 and Fig. 12.

ANALYSIS OF RESULTS AND COMPARISON WITH THEORY

Bubble Rise Velocity in Still Water

A constant rise velocity independent of length is to be expected from the experimental results and theory of both G. I. Taylor and Dumitrescu for cases where wall shear stresses are negligible. The pressure boundary condition on the bubble surface is the same in all cases and eddies behind the bubble have negligible effect upon the smooth character of the flow around the bubble itself. One might think that shear stresses would slow down the water flow around the bubble which would be expected to rise slightly slower in consequence. In fact, the observed tendency is for longer bubbles to rise slightly faster than the shorter ones so presumably the problem is not a simple one.

Laird and Chisholm (3) in an experimental investigation in a 2" diameter tube claim an increase of about 10% in bubble rise velocity as the length is increased from some 2 diameters to 25 diameters. In our experiments, no changes of such magnitude were observed, perhaps because no bubbles of over 12 diameters in length were timed. Variations in rise velocity we found were no more than 2 or 3%, while Laird and Chisholm's data shows considerable spread in this region. Because of the method of admitting the air into the tube used by Laird and Chisholm, one might expect the fluid to be still moving rather than stationary when the bubble arrived, which motion would also affect the rise velocity. This motion may well be more pronounced for the longer bubbles.

Variation of Rise Velocity with Water Velocity and Viscosity

Two qualitative results are immediate from a study of Fig. 3. The bubble relative velocity increases as the water velocity increases and increases more rapidly in the more viscous, colder liquid. The second result seems surprising.

In an attempt to rationalize the results the constant C of Taylor and Dumitrescu was split up into two parts, C_1 and C_2. C_1 is the governing coefficient in static water when C_2 is by definition unity. C_2 is a function of

water velocity, thus:

$$V_b = C_1 C_2 \sqrt{g D} \tag{9}$$

A plot of C_1 against bubble Reynolds number ($Re_b = \frac{V_b D}{\nu}$), (Fig. 13), using both the results of these experiments and Dumitrescu's gives an excellent smooth curve which rapidly tends to a constant value within less than 1% of Dumitrescu's theoretical results for C_1. It seems rational to plot against bubble Reynolds' number as it would be a measure of the departure of the fluid from ideal potential flow. Dumitrescu originally plotted against a dimensionless parameter involving surface tension, presumably arguing that surface tension will change the bubble shape at the nose in small diameter pipes. We prefer Reynolds' number since the water dynamics appear to be the governing factor.

Rationalization of the variation of C_2 is more difficult. Obviously, both V_b, V_w, and $V_b + V_w$ are important parameters for determining the velocity profiles and shear stresses. Fig. 15 shows how the velocity profile of the oncoming water changes relative to the bubble. Wall shear stresses acting on the water which runs down around the bubble are less in the upflow case because the mean flow velocity must be subtracted from the velocities calculated relative to the bubble in order to calculate absolute flow velocities. Thus, the wall shear stress also tends to increase bubble velocities in the case of upflow. Presumably the potential flow solution is wrong when the oncoming velocity profile is not uniform. In the case of upflow, the profile as seen by the bubble (Fig. 14), is already partly distorted in the direction necessary to pass the bubble; hence, we might expect greater flow rates around the bubble and a higher rise velocity. Analysis of such a problem would be complex, but could be attempted by a variation of Dumitrescu's method.

Since the oncoming velocity profile and the nature of the flow around the bubble are determined by Reynolds' number, it seems logical to try a correlation plot on this basis. There are only two independent Reynolds

numbers for long bubbles. These could be taken as the one for the stream and that for the bubble. The plot which gave best results is shown in Fig. 15. Points were found to fall in the "laminar line" to a good degree of accuracy for bubble Reynolds numbers below 3000. For the bubble Reynolds numbers between 3000 and 5000 results do not coordinate well and are scattered around in a general area of the graph, presumably a transition region where turbulent flow is starting to be initiated. At higher bubble Reynolds numbers, results are again more consistent but with the present apparatus it was impossible to explore the fully developed turbulent region properly. It seems logical, though, that as the velocity profile becomes flatter at large Reynolds number, C_2 should approach 1. This appears to be the case.

There is a suggestion of transition phenomena in the main water flow, i.e. dependent on Re_w, and this obscures the results of the other transition determined by Re_b.

It is unfortunate that most of these experiments cover the regions of transition flow phenomena, since this makes a correlation of the data more difficult. The results for totally laminar flow are consistent and reliable. The results for $Re_b > 3000$ are average curves which may be used for practical purposes with some approximation, certainly giving better results than the assumption that C_2 is constant and unity.

In the case of practical interest when a string of bubbles follow one another, other effects such as slug length Reynolds number and wake velocity profiles, may also become important.

BUBBLE STABILITY

In general, the shape was very stable and the bubble proceeded up the pipe as if it were a solid object. No satisfactory explanation or theory was formed for the bubble instability which was observed for downflow. It is also unknown as yet whether such instability could occur for upflow in very large pipes or if a reversed water flow is essential.

ANALYSIS OF PRESSURE DROP RESULTS

In Appendix 2 are shown the results of pressure drop measurements compared with theoretical predictions using equations (5) and (7) and the results of the previous experiments for the appropriate value of V_b.

For the 1" pipe, in which shear stresses are small, the results agree excellently with theory. Deviations greater than 1% are only found at the highest flow rates and may be attributed to the influence of shear stress.

For the 3/4" pipe the agreement is not so good, as was to be expected. In fact, the error changes sign as the water flow is increased. For low flow rates at sufficiently high quality the dominant shear stresses act on the stream running down between the bubble and the wall and the general effect is to support the water column and so decrease the pressure drop. For these conditions the effect of shear stress is, strangely enough, to provided an internal force in the direction of mean flow. At higher flow rates the absolute velocity of the water running down the bubble becomes reversed in the directions of mean flow and this effect, together with the usual shear stresses acting on the plug of water between bubbles, results in an eventual increase in pressure drop above that predicted by potential flow theory.

SUMMARY

For convenience, the method of calculating slug flows is summarized here. The time average pressure gradient neglecting wall shear stress is

$$\frac{\Delta P}{\Delta L} = \rho_a g = g \rho_f \left[\frac{Q_f + V_b A_p}{Q_f + Q_g + V_b A_p} \right] + \frac{g \rho_g Q_g}{Q_f + Q_g + V_b A_p} \qquad (5)(7)$$

$$V_b = C_1 C_2 \sqrt{g D_p} \qquad (9)$$

in which C_1 and C_2 are evaluated from Figures (13) and (15).

The slug length can be obtained from Figure (12). The bubble length can then be obtained from

$$L_b = \frac{Q_g L_s + n (D_p)(Q_g + Q_f + V_b A_p)}{m(Q_g + Q_f + V_b A_p) - Q_g} \qquad (8)$$

As long as the shape can be approximated by the shape that would exist in a potential flow

$$m = 0.913$$
$$n = 0.526$$
$$\text{for } 2 < L_b/D_p < 20$$

The period of the pressure fluctuations is approximately

$$\Delta t = \frac{(L_s + L_b) A_p}{Q_f + Q_g + V_b A_p} \qquad (1)$$

The magnitude of the pressure fluctuations is approximately

$$\Delta(\Delta P) = L_s g \rho_f \qquad (10)$$

for taps which are more than one slug length apart.

Laird and Chisholm give results for apparent wall shear stress versus bubble length for one particular size of pipe and with stagnant water. Their shear losses increased as bubble length to the 1.5 power. In the present case, a detailed analysis of the shear stress effects, which would have to take into

account the detailed water velocity profiles around the bubbles and in the wake, has not been attempted although results can be explained qualitatively.

With the 1/2" pipe, the range of flow rates is more limited because of the previously mentioned problem of "bowlerhat" bubbles. The observed pressure drop is always in excess of the theoretical. Shear stresses act predominately downwards on the flowing fluids. They are of considerably higher importance than is the case of the larger pipes because of higher velocities coupled with smaller pipe diameter.

BUBBLE AND SLUG LENGTHS

The most valuable results of these experiments were obtained with the 1/2" pipe. This is due to the greater completeness of the data in view of the fact that one camera frame often covered a range of several bubble lengths. In the case of the 1" pipe often only part of the pattern was visible.

Results for the 1/2" pipe are shown in histogram form in Figure (11). The spread in bubble lengths is considerable. Slug lengths are more regular, both over one experimentaand from one experiment to the next. This result is to be expected in view of the fact that the limiting process in determining bubble lengths is an agglomeration process determined by the velocity profiles in the bubble wake. After slugs reach a certain length the attraction between bubbles becomes very small and a fairly regular slug length is obtained. For higher flow rates where shear stresses and turbulence are considerable both bubble and slug lengths become steadily less regular.

Slug and bubble lengths are related to each other via flow rates and bubble rise velocity as in equation (9). Slug length is a useful parameter to quote because of its relative invariance. Maximum and minimum mean slug lengths for various flow rates in a given pipe are shown against pipe diameter in Figure (12). Further and more detailed data is needed to make possible ananalysis in terms of wake dynamics.

Note that actual bubble length may be less than the theoretical calculated from continuity considerations becsuse of the air volume associated with the small bubbles in the wake.

Attraction Between Bubbles

Figure (16) shows the probable velocity distributions in the wake of a bubble. A following bubble which is influenced by the wake will see a higher water approach velocity near the wall. This tends to increase the flow around the bubble and, hence, its rise velocity. The magnitude of the effect is probably a function of length-diameter ratio in the wake and Reynolds number at the tail of the preceding bubble.

CONCLUSIONS

1) Entrance effects can persist for great lengths, L/D = 300, and long times, in developing two phase flows.

2) Wall shear stresses at moderate and low velocities contribute only slightly to the pressure drop in slug flows.

3) Bubble rise velocities in slug flow are quite sensitive to the velocity profile in the water ahead of the bubbles. The effect of wall shear stress manifests itself primarily through the velocity profiles.

4) Pressure drop, density, slug length, bubble length and fluctuation pressure drops and frequencies can be calculated for fully developed slug flow with good accuracy.

Acknowledgements

This work has been entirely supported by the Office of Naval Research and has been performed in the Heat Transfer Laboratory of the Massachusetts Institute of Technology, which is under the direction of W. M. Rohsenow.

Bibliography

1. Dumitrescu, D. T., "Strömung an einer Luftblase im senkrechten Rohr", ZAMM, 1943, Vol. 23, No. 3, pp. 139-149.

2. Davis, R. M. and G. I. Taylor, "The Mechanics of Large Bubbles Rising Through Extended Liquids and Through Liquids in Tubes", Proc. Roy. Soc., London, 1950, Vol. 200, Series A, pp.375-390.

3. Laird, A. D. K. and Chisholm, "Pressure and Forces Along Cylindrical Bubbles in a Vertical Tube", Indus. and Eng. Chem., 48 (8), August 1956, pp. 1316-18.

Captions

Figure 1

Figure 2 Main features of the apparatus

Figure 3 Bubble velocity V_b against average water velocity V_w in ft/sec

_____ 1" pipe with cold water

__ __ __ 1" pipe with hot water

_____ 3/4" pipe with cold water

__°__·__°__ 3/4" pipe with hot water

-·-·-·-·-·-·- 1/2" pipe with cold water

x denotes onset of bubble instability as described in the text

Figure 4 $Q_a = 0.073$ $Q_f = 0$ in CFM pipe diameter 1 inch

Typical low speed flow. Bubbles are short and smooth and have short wakes. A and C show stages in the agglomeration process. The lower bubble is caught in the wake of the upper, distorts, and accelerates rapidly.

Figure 5 $Q_a = 0.160$ $Q_f = 0$ in CFM pipe diameter 1 inch

Long, smooth bubbles. B shows a rare case of interaction of a large bubble with a cloud of small bubbles. The bubble surface becomes very distorted and the wake turbulent.

Figure 6 $Q_a = 0.208$ $Q_f = 0.288$ (in CFM) pipe diameter 1 inch

Photographs of entrance effects some 200 diameters from inlet. The small bubbles are in the process of agglomeration to form small G. I. Taylor bubbles.

Figure 7 $Q_a = 0.322$ $Q_f = 0.288$ (in CFM) pipe diameter 1 inch

Turbulent bubbles with turbulent wakes. The water slugs are full of small bubbles. Theoretical predictions for pressure drop (based on smooth potential flow theory) begin to lose accuracy

Figure 8 $Q_a = 0.126$ $Q_f = 0.118$ (in CFM) pipe diameter 1/2 inch

"Rough bubbles". These are formed by the agglomeration of many smaller bubbles (originally of Bowler Hat shape), but local surface tension forces inhibit complete unification and the result is a stack of bubbles past which flow is very turbulent

Figure 9 $Q_a = 0.165$ $Q_f = 0.119$ (in CFM) pipe diameter 1/2 inch

A mixture of smooth and rough bubble shapes. The rough form changes more rapidly into the smooth form as flow velocities are increased

Figure 10 $Q_a = 0.304$ $Q_f = 0.124$ (in CFM) pipe diameter 1/2 inch

Long, smooth bubbles, sometimes capped by a smaller bubble, with a large number of small bubbles in the wake

Figure 11 Histogram results for bubble and slug lengths in 1/2" diameter pipe

A. $Q_g = 0.136$ $Q_f = 0.118$ Mean $L_b = 3.67"$ Mean $L_s = 3.02"$

B. $Q_g = 0.165$ $Q_f = 0.119$ Mean $L_b = 4.48"$ Mean $L_s = 3.14"$

C. $Q_g = 0.192$ $Q_f = 0.117$ Mean $L_b = 4.95"$ Mean $L_s = 3.12"$

D. $Q_g = 0.252$ $Q_f = 0.118$ Mean $L_b = 6.40"$ Mean $L_s = 3.38"$

E. $Q_g = 0.304$ $Q_f = 0.124$ Mean $L_b = 8.21"$ Mean $L_s = 3.90"$

F. $Q_g = 0.294$ $Q_f = 0.272$ Mean $L_b = 5.47"$ Mean $L_s = 4.68"$

G. $Q_g = 0.289$ $Q_f = 0.262$ Mean $L_b = 5.31"$ Mean $L_s = 4.74"$

Figure 12 Range of mean slug lengths as a function of pipe diameter for various flow rates of the two phases

Figure 13 Dimensionless constant C_1 against bubble Reynolds number

x Results of Dumitrescu

0 Results of Griffith and Wallis

Dumitrescu's theory gives $C_1 = 0.350$ for potential flow. G. I. Taylor in a more approximate analysis obtains $C_1 = 0.328$

Figure 14 Oncoming water velocity profiles relative to a rising bubble

Figure 15 Coefficient C_2 against liquid Reynolds number for various values of bubble Reynolds number

———	"Laminar"	$N_{Re_b} = 0 \rightarrow 3000$
— — —	"Transition"	$N_{Re_b} = 4000$
—·—·—	"Transition"	$N_{Re_b} = 5000$
———	"Transition"	$N_{Re_b} = 6000$
—··—··—	"Turbulent"	$N_{Re_b} = 7000$
—·—·—	"Turbulent"	$N_{Re_b} = 8000$

Figure 16 Velocity profiles in bubble wake relative to a following bubble. Water flow upwards

List of Symbols

A_w Wall area

A_p Pipe area

Q_f Liquid flow rate

Q_g Gas flow rate

V_b Bubble rise velocity with respect to the liquid ahead of the bubble

V_w Mean water velocity

$\mathcal{V}_b, \mathcal{V}_f, \mathcal{V}_g, \mathcal{V}$ Bubble volume, liquid volume, vapor volume and total volume

L_s Slug length

L_b Bubble length

P Pressure

L Length

ρ_a Average density

ρ_g Gas density

ρ_f Liquid density

τ_w Wall shear stress

m Dimensionless constant relating bubble volume to length in Eq. 8 equal to (.913) for potential flow

n Dimensionless constant relating bubble volume to length in Eq. 8 equal to (.526) for potential flow

C_1, C_2 Dimensionless constants used to calculate gubble rise velocities from equation 9. To be evaluated from Figures (13) and (15)

$$N_{Re_b} = \frac{V_b \rho_f D_p}{\mu_f}$$, Bubble Reynolds number

$$N_{Re_f} = \frac{\left(\frac{Q_f + Q_g}{A_p}\right) D_p \rho_f}{\mu_f}$$, liquid Reynolds number

APPENDIX 1

Data of bubble rise velocities

1/2" pipe

V_b f.p.s.	V_w f.p.s.	Temperature ^oC	N_{Re_b}	N_{Re_w}
0.344	0.	10	1070	0
0.353	0.065	10	1100	200
0.354	0.093	10	1100	290
0.399	0.205	10	1240	640
0.409	0.220	10	1270	680
0.458	0.542	10	1420	1680
0.52	0.983	10	1620	3050
0.342	0	10	1060	0
0.323	-0.082	10	1000	250
0.303	-0.186	10	940	580
0.287	-0.261	10	890	810
0.293	-0.293	10	910	910
0.274	-0.365	10	850	1130
0.239	-0.421	10	740	1310
0.216	-0.496	10	670	1540
0.228 0.210	-0.840	10	710 650	2610
0.22	-1.58	10	680	4900

APPENDIX 2

Pressure drop data

1/2" pipe

Q_g CFM	Q_f CFM	Superficial Velocity $(\frac{Q_g + Q_f}{A_p})$ f.p.s.	$\Delta p/\Delta L$ Observed	$\Delta p/\Delta L$ Theoretical	Observed L_B in	Observed L_S in
0.136	0.118	3.1	0.695	0.556	3.67	3.02
0.165	0.119	3.5	0.630	0.510	4.48	3.14
0.192	0.117	3.8	0.615	0.469	4.95	3.12
0.252	0.118	4.5	0.561	0.410	6.40	3.38
0.304	0.124	5.2	0.53	0.373	8.21	3.90
0.296	0.262	6.8	0.900	0.527	5.47	4.68
0.294	0.272	6.9	0.917	0.530	5.31	4.74

3/4" pipe

0.046	—	.25	0.638	0.707		
0.080	—	.43	0.517	0.604		
0.125	—	.68	0.420	0.511		
0.201	—	1.09	0.302	0.411		
0.321	—	1.74	0.145	0.313		
0.053	0.050	.56	0.730	0.770		
0.084	0.049	.72	0.642	0.684		
0.134	0.048	.99	0.542	0.583		
0.116	0.119	1.27	0.700	0.708		
0.192	0.124	1.71	0.580	0.589		
0.341	0.128	2.54	0.430	0.454		
0.265	0.264	2.87	0.67	0.62		
0.387	0.261	3.51	0.56	0.53		
0	0.261	1.48	0.015	0		

1" pipe

0.073	—	.22	0.750	0.745	5.65	10
0.094	—	.29	0.712	0.704	6.3	13
0.124	—	.37	0.658	0.652	8.1	13
0.160	—	.49	0.607	0.602	10.7	15
0.078	0.124	.62	0.835	0.828	2.9	10.5
0.098	0.122	.67	0.803	0.793	3.6	13
0.127	0.124	.77	0.758	0.750	4.8	13
0.166	0.126	.89	0.702	0.700	6.5	10.5
0.209	0.127	1.03	0.653	0.653	8.2	15
0.208	0.288	1.51	0.765	0.735	~1	—
0.322	0.288	1.87	0.663	0.645	6.5	10
0.463	0.293	2.31	0.577	0.560	9.8	13

3/4" pipe

V_b ft/sec	V_w ft/sec	Temperature °C	N_{Re_b}	N_{Re_w}
0.481	0	10	2250	0
0.506	0.043	10	2370	200
0.546	0.121	10	2550	570
0.550	0.128	10	2570	600
0.579	0.214	10	2710	1000
0.609	0.273	10	2850	1280
0.637	0.346	10	2980	1620
0.666	0.431	10	3120	2010
0.666	0.487	10	3120	2280
0.657	0.593	10	3070	2770
0.749	0.918	10	3500	4300
0.461	-0.023	10	2150	110
0.439	-0.072	10	2060	340
0.420	-0.115	10	1960	540
0.405	-0.197	10	1890	920
0.392	-0.197	10	1830	920
0.389 0.394	-0.232	10	1820 1840	1080
0.412	-0.294	10	1930	1370
0.443	-0.443	10	2030	2030
0.676	0.435	11	3200	2060
0.578	0.204	16	2960	1050
0.585	0.487	23.5	3500	2900
0.578	0.219	24.5	3500	1300
0.576	0.508	34	4230	3740
0.542	0.178	37	4300	1390
0.533	0.129	38	4300	1030
0.523 0.513	0.079	38	4200	630
0.551 0.537	0.206	39	4300	1670
0.556 0.504	0.262	42	4500	2200
0.588 0.578	0.370	44	5100	3300
0.606 0.620	0.519	48	5600	4800
0.497	0	47	4500	0
0.447 0.450	-0.230	47	4100	2080
0.406	-0.406	50	3800	3800

1" pipe

V_b ft/sec	V_w ft/sec	Temperature	N_{Re_b}	N_{Re_w}
0.577	0	10	3600	0
0.685	0.224	10	4300	1390
0.707	0.385	10	4400	2400
0.708	0.508	10	4400	3200
0.785	0.793	10	4900	4900
0.81	0.99	10	5000	6100
0.529	-0.052	10	3300	320
0.520	-0.098	10	3200	610
0.546 0.526	-0.143	10	3300	880
0.615	0.144	34	6200	1430
0.634	0.232	37	6500	2400
0.640	0.307	39	6900	3300
0.615	0.135	39	6600	1400
0.669	0.442	45	7900	5200
0.577	0	49	7200	0
0.676	0.556	49	8400	6900

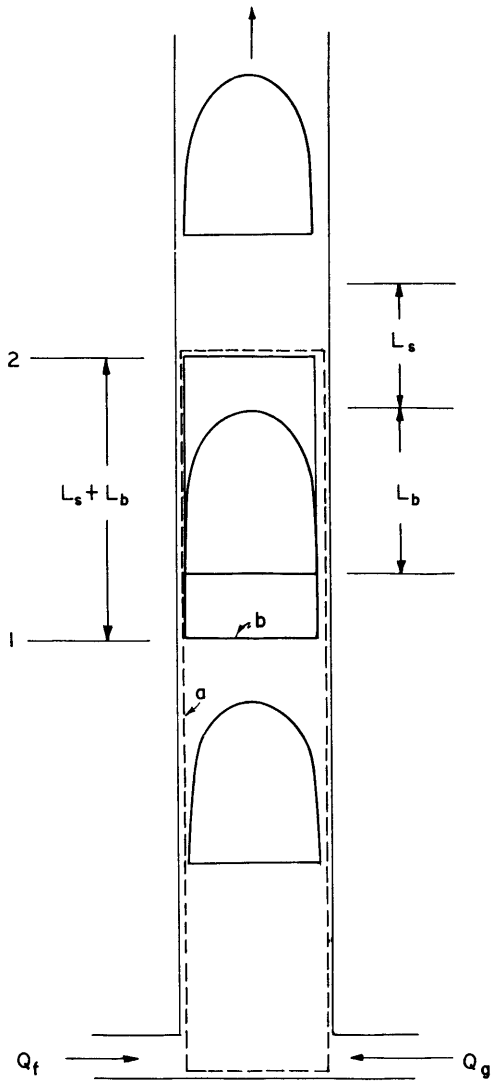

FIG. 1

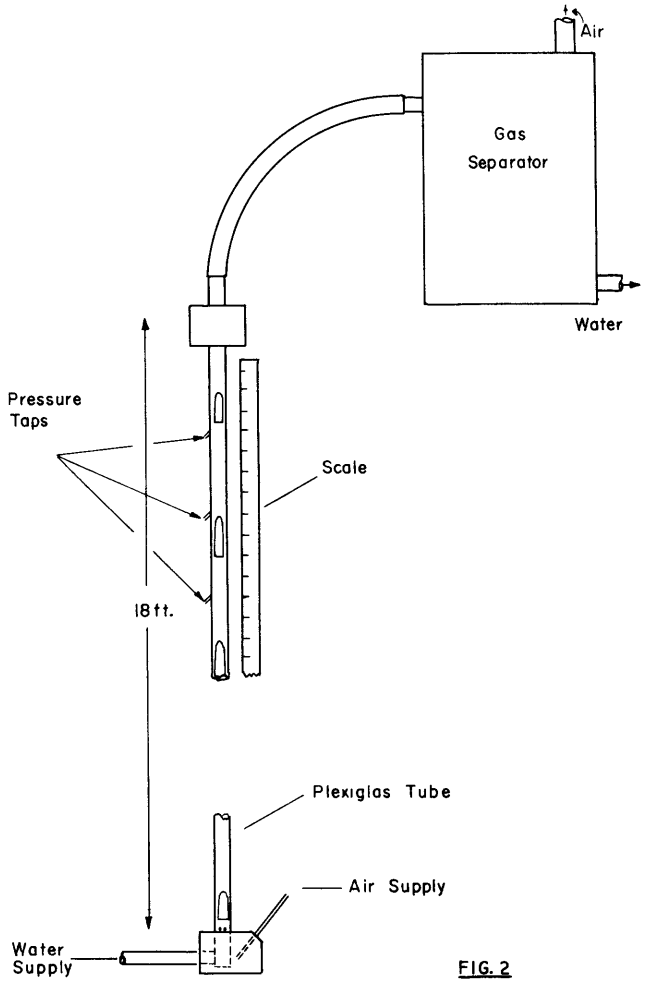

FIG. 2

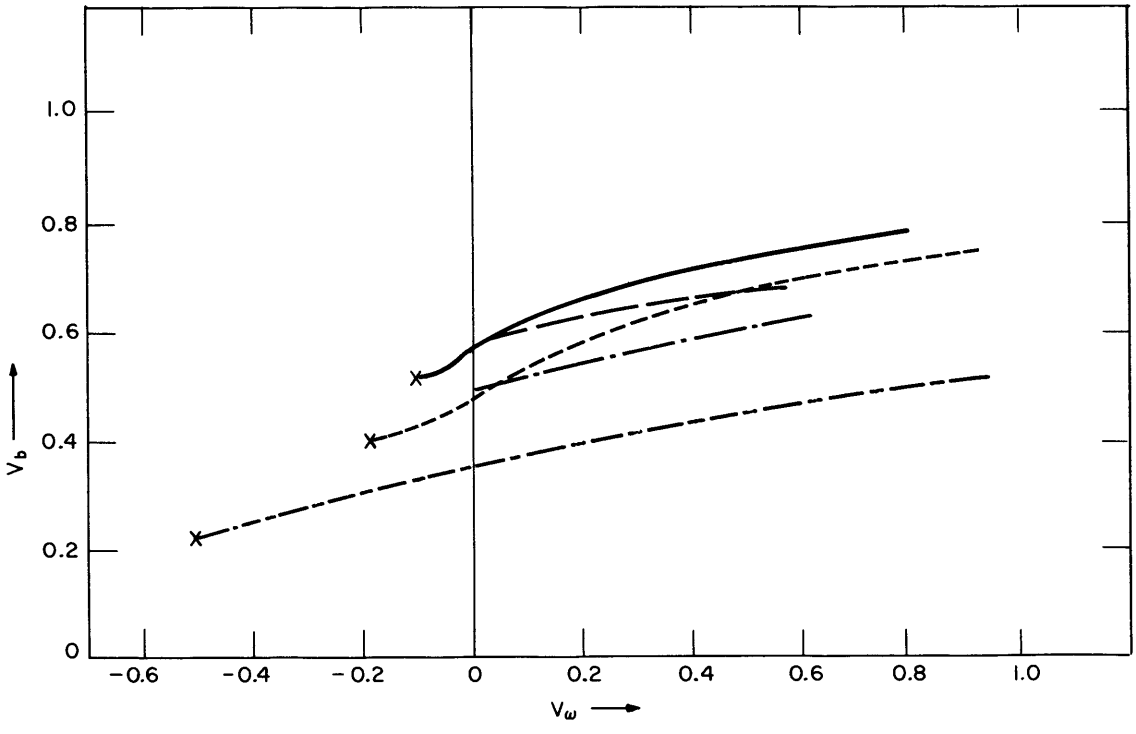

FIG. 3

A B C D

FIG. 4

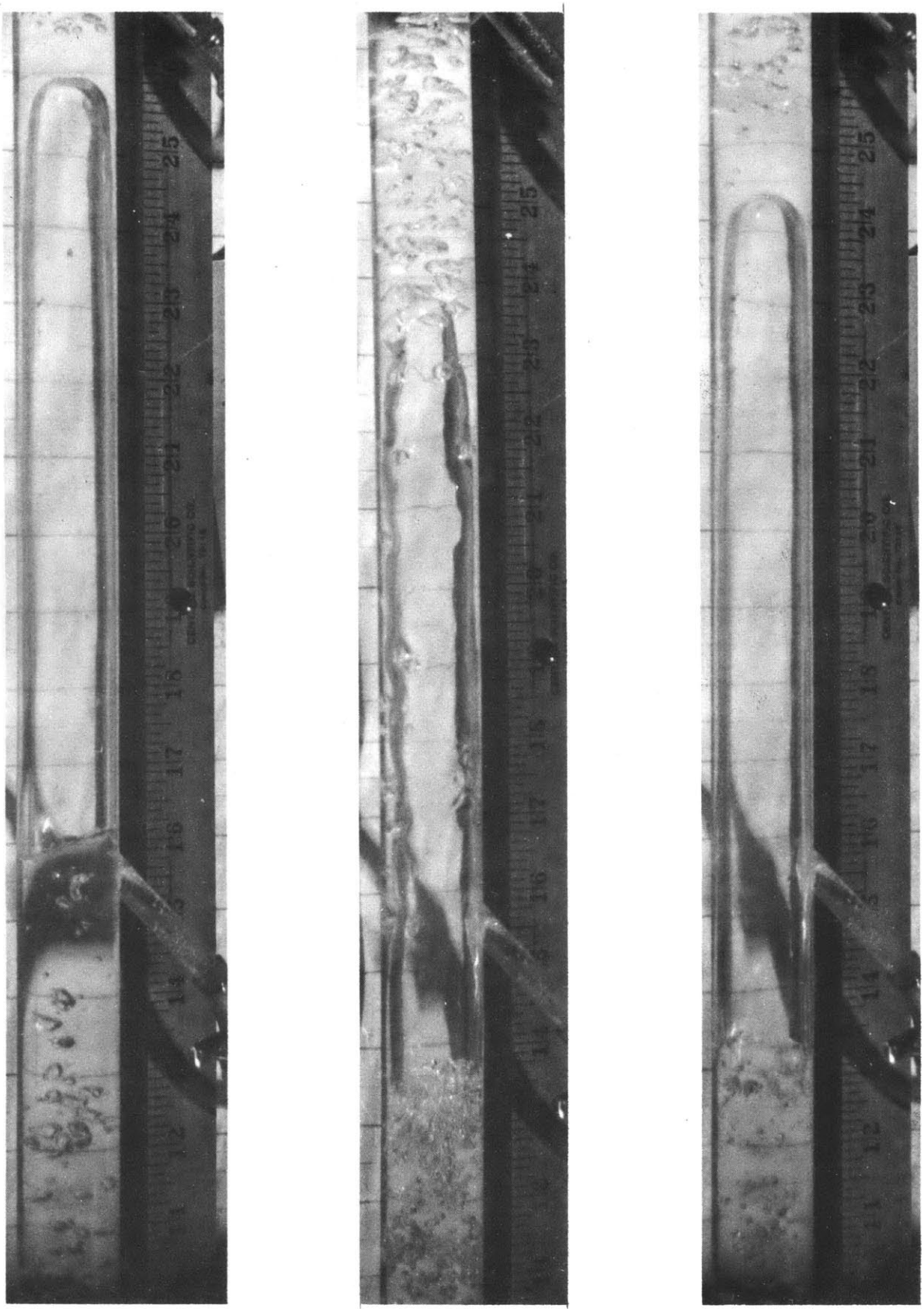

A B C

FIG. 5

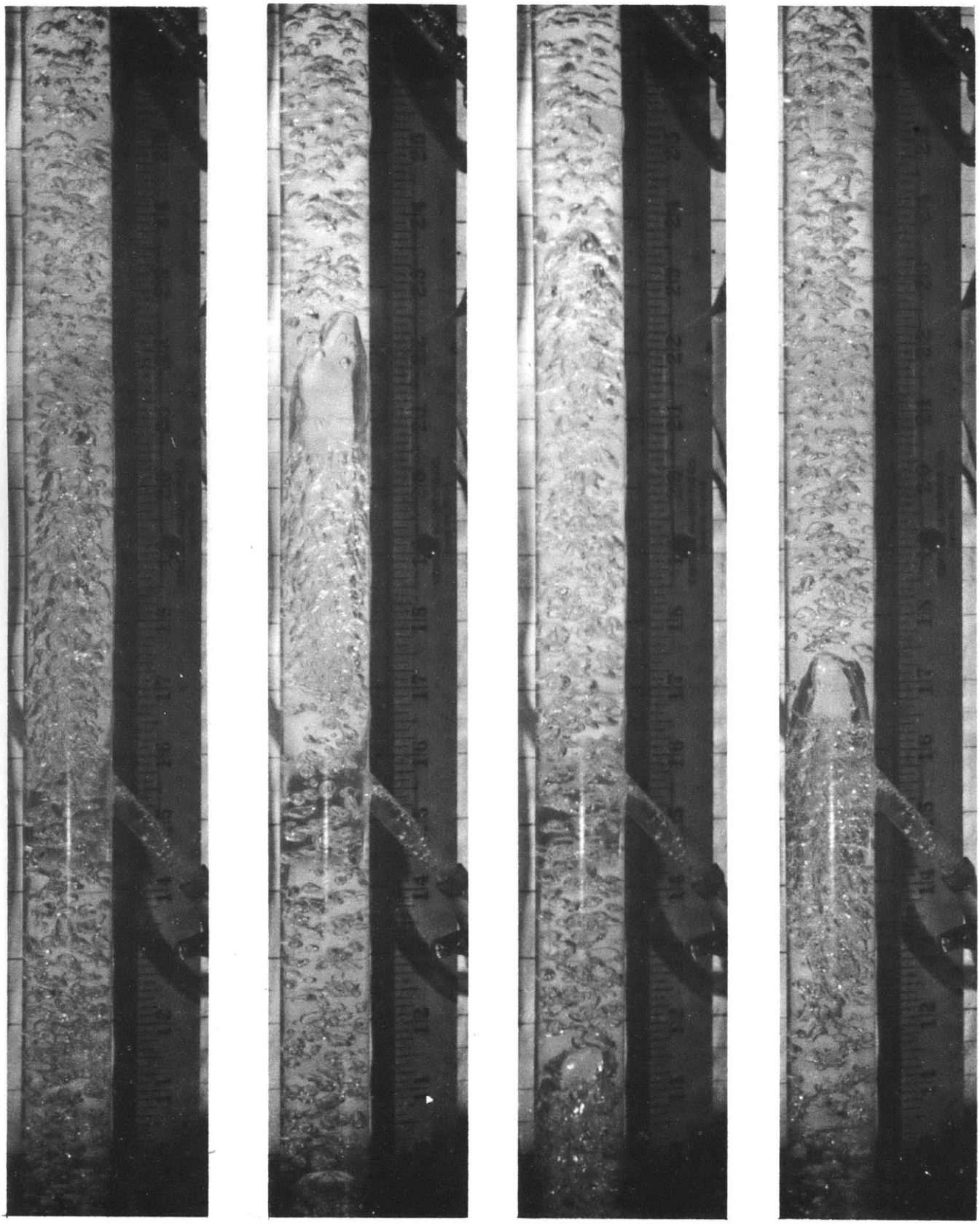

A B C D

FIG. 6

A B C D

FIG. 7

A B C D

FIG. 8

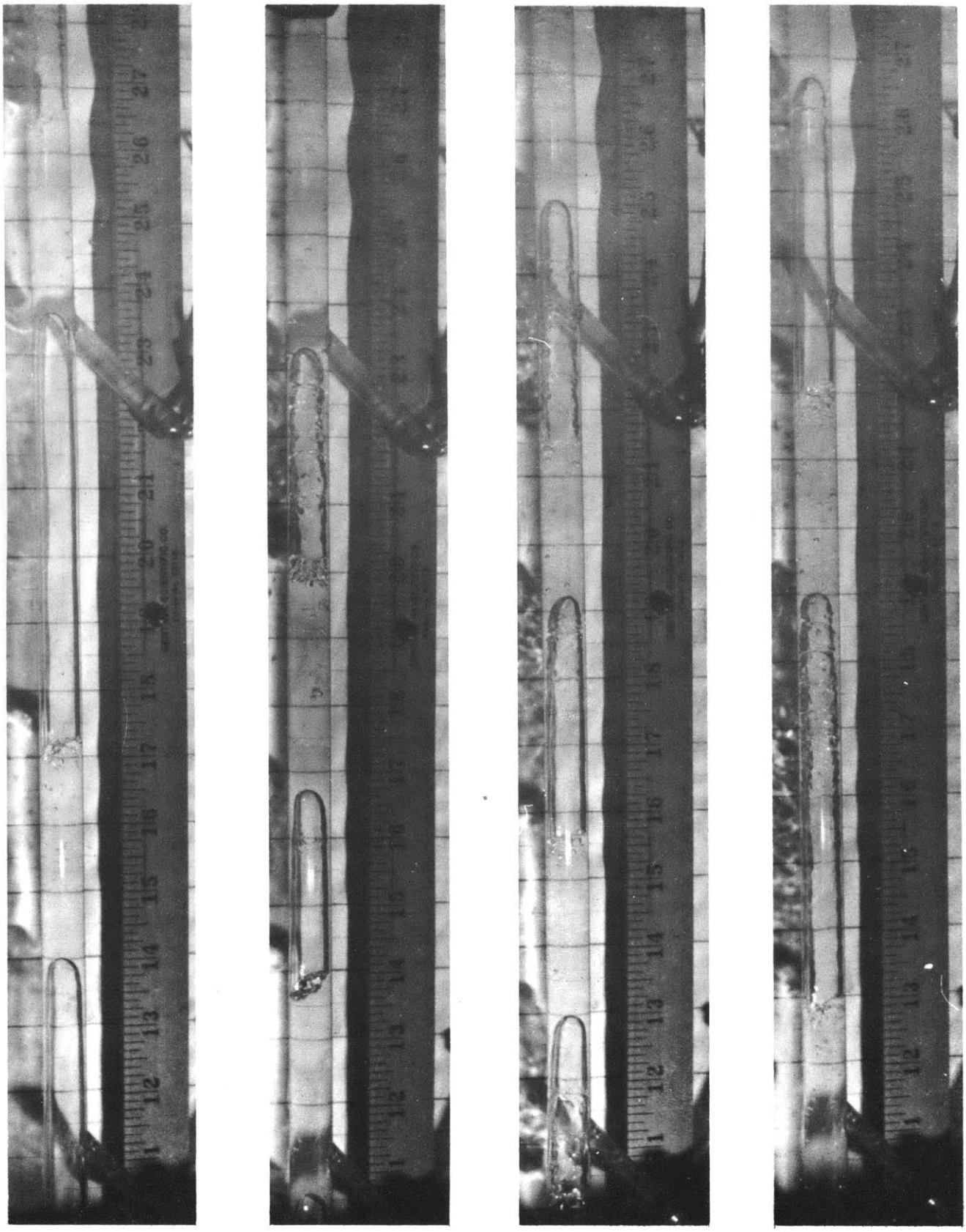

A B C D

FIG. 9

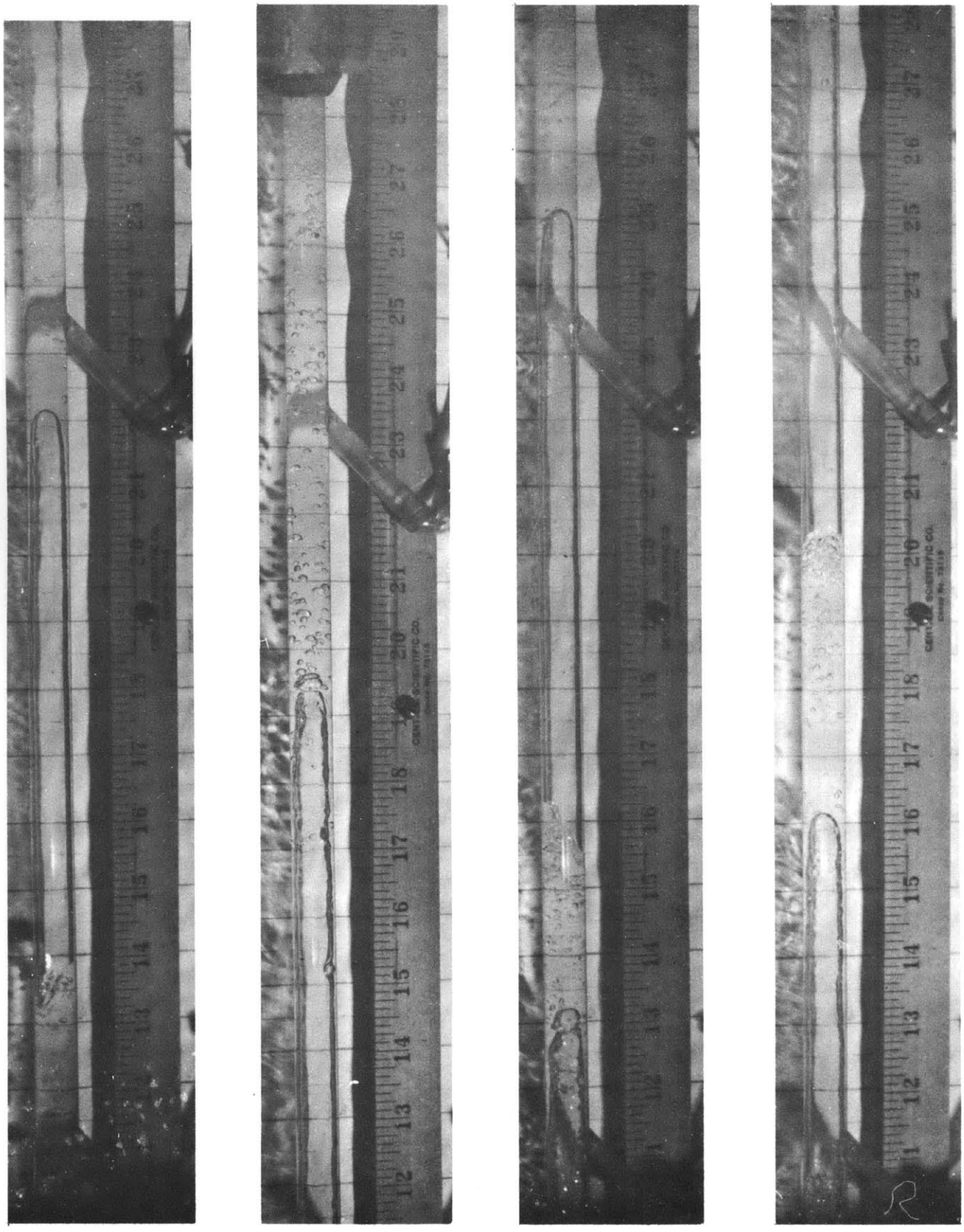

A B C D

FIG. 10

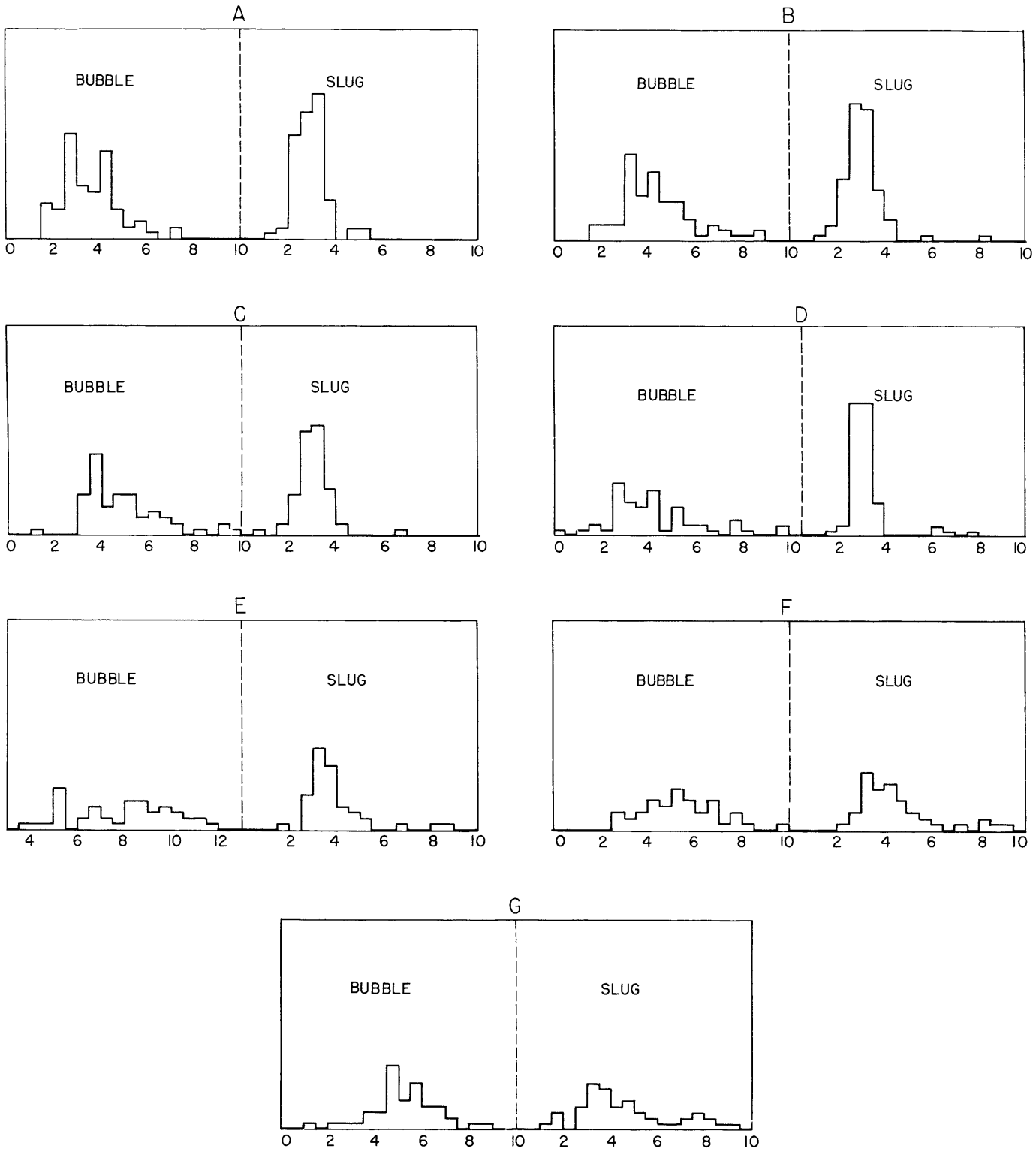
A
BUBBLE
SLUG
0 2 4 6 8 10 2 4 6 8 10
B
BUBBLE
SLUG
0 2 4 6 8 10 2 4 6 8 10
C
BUBBLE
SLUG
0 2 4 6 8 10 2 4 6 8 10
D
BUBBLE
SLUG
0 2 4 6 8 10 2 4 6 8 10
E
BUBBLE
SLUG
4 6 8 10 12 2 4 6 8 10
F
BUBBLE
SLUG
0 2 4 6 8 10 2 4 6 8 10
G
BUBBLE
SLUG
0 2 4 6 8 10 2 4 6 8 10

FIG. 11

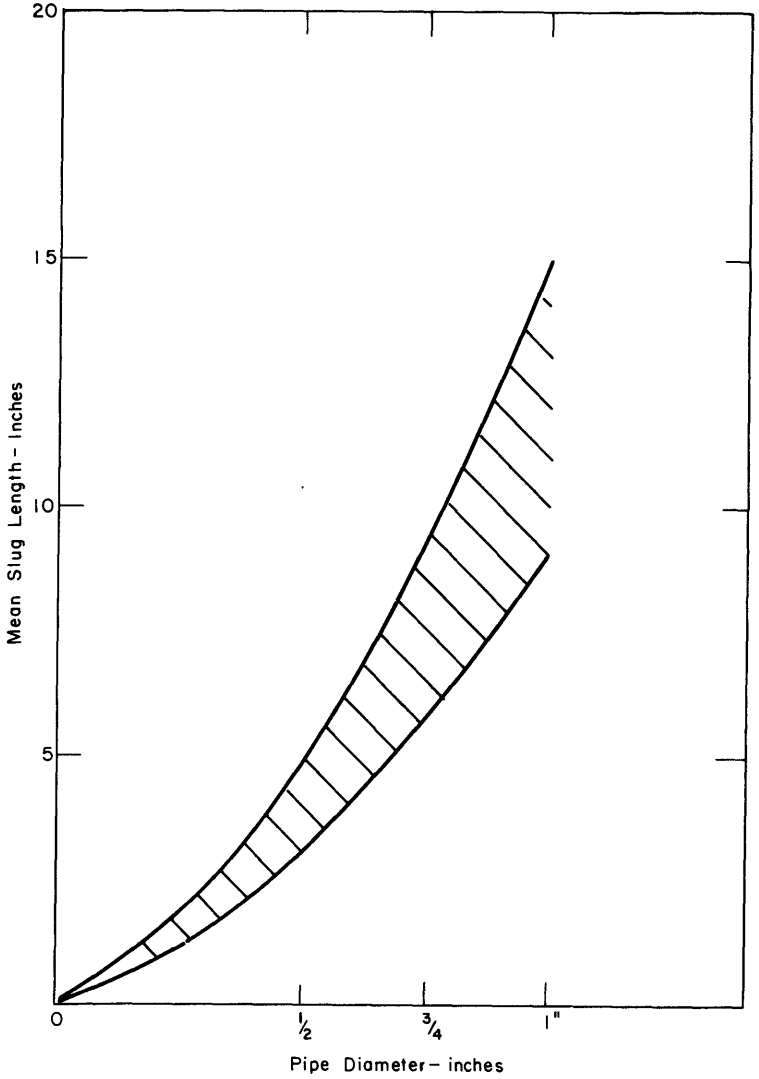

FIG. 12

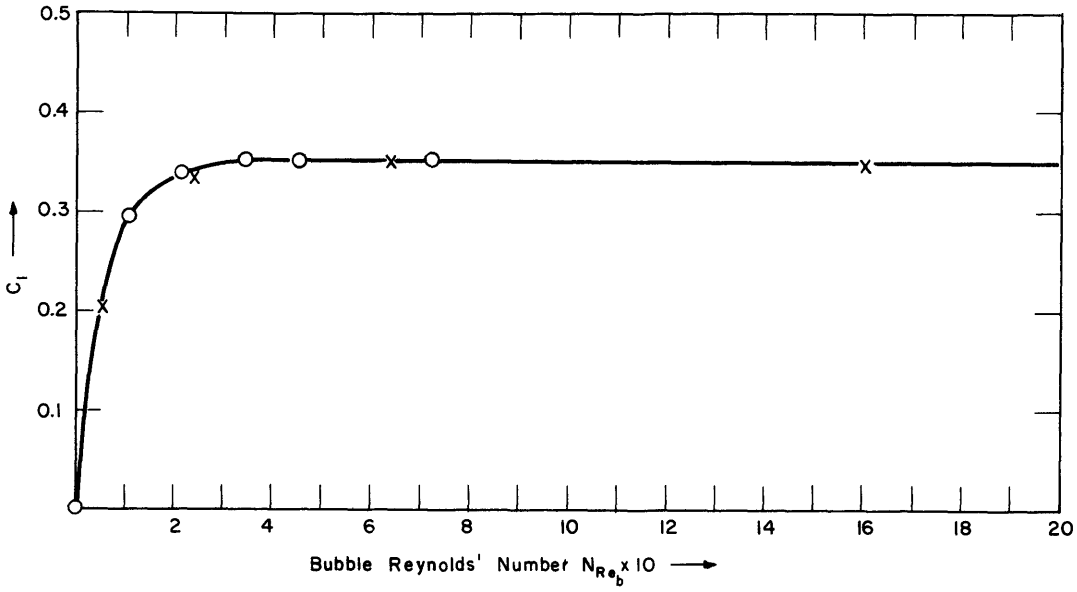

FIG. 13

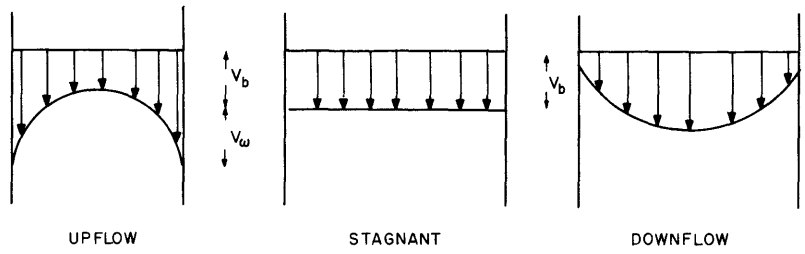

FIG. 14

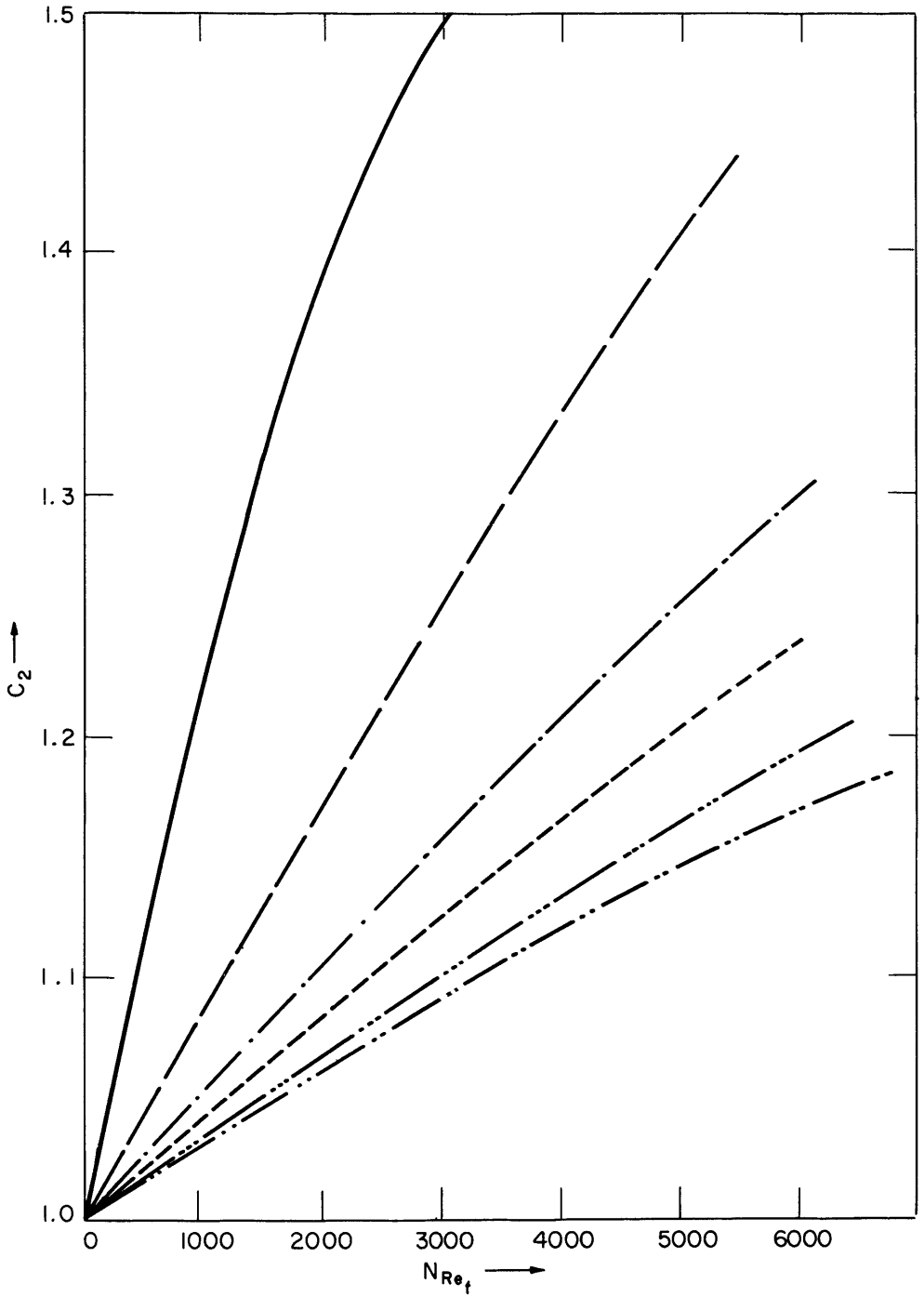

FIG. 15

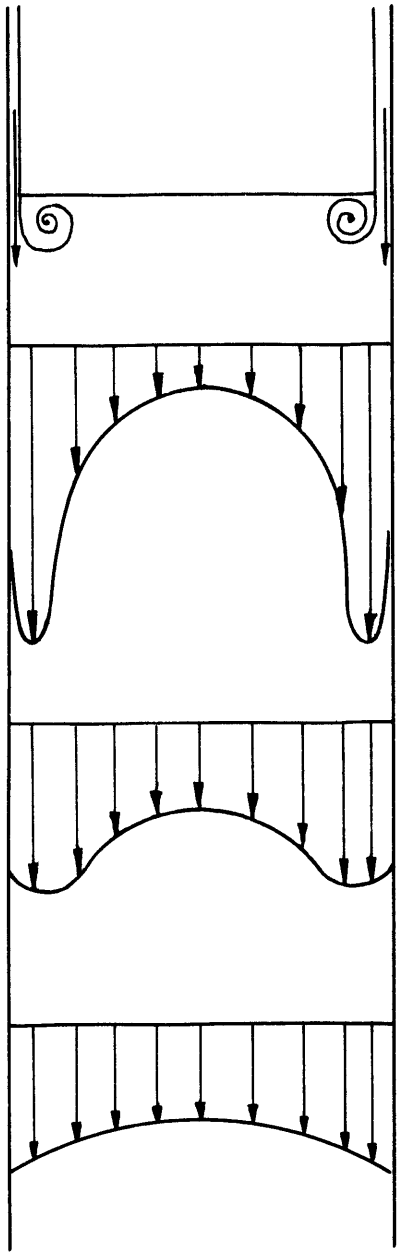

FIG. 16